Multilayer partially reflective surfaces for broadband fabry-perot cavity antennas

Konstantinidis, Konstantinos; Feresidis, Alexandros P.; Hall, Peter S.

DOI:
10.1109/TAP.2014.2320755

Multi-layer Partially Reflective Surfaces for Broadband Fabry-Perot Cavity Antennas

Konstantinos Konstantinidis, Alexandros P. Feresidis, *Senior Member, IEEE* and Peter S. Hall, *Fellow, IEEE*

***Abstract*— A high gain broadband Fabry-Perot type antenna is proposed, based on multi-layer periodic Partially Reflective Surfaces (PRSs). Three layers of PRSs are employed, consisting of metallic patches printed on thin dielectric substrates and placed in front of a ground plane, forming three open cavities. The antenna performance is based on the reflection characteristics of the PRS array, which are obtained using periodic analysis. An equivalent circuit approach is presented for the design of the multi-layer PRSs showing very good agreement with full-wave analysis. The geometry has been optimized using full wave simulations (CST Microwave Studio™). An antenna of around 20 dBi gain at an operating frequency of 14.5 GHz is obtained with a 3dB bandwidth of about 15%, outperforming earlier antenna designs based on two-layer PRS. A prototype has been fabricated and tested, validating the simulation results.**

***Index Terms*— Broadband antennas, Fabry–Perot cavities (FPC), high–gain, leaky wave antennas, partially reflective surface (PRS), periodic structures**

I. Introduction

FABRY-PEROT cavity (FPC) type antennas employing doubly periodic arrays of conducting elements, or apertures in a conducting sheet, have been widely investigated in the past, [1, 2], as they provide high-gain performance, high efficiency and low-complexity feeding network compared to conventional microstrip patch arrays [3]. Antennas of this type find numerous applications in modern communications, radar and sensor systems. They consist of a metallic or metallo-dielectric periodic array placed at approximately half wavelength distance over a metallic ground plane and a low-directivity primary source (e.g. dipole). The passive array acts as a Partially Reflective Surface (PRS), [1, 2], creating a Fabry-Perot type resonant cavity that significantly increases the gain and directivity of the primary source [4-6]. A ray optics approximation can be used to describe the antenna operation by means of the multiple reflections between the ground plane and the PRS [1, 2]. A leaky-wave approach has also been successfully employed in order to analyse and design this type of antennas [5-7]. In [8-10], planar artificial magnetic conductor (AMC) ground planes have been introduced as means to reduce the profile of such antennas from half-wavelength to sub-wavelength values.

Manuscript received June 13, 2013; revised October 1, 2013. This work was supported by the UK EPSRC under Grant EP/J500367/1. A. P. Feresidis wishes to acknowledge the support by the Royal Academy of Engineering and The Leverhulme Trust under a senior research fellowship.

K. Konstantinidis, A. P. Feresidis and P. S. Hall are with the School of Electronic, Electrical and Computer Engineering, University of Birmingham, Edgbaston, Birmingham B15 2TT, U.K.

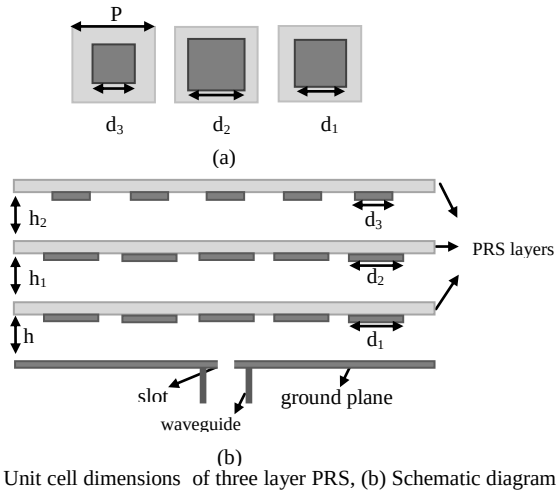

Fig. 1. (a) Unit cell dimensions of three layer PRS, (b) Schematic diagram of the proposed antenna.

However, FPC antennas have inherently narrow operational bandwidth. A technique for enhancing the bandwidth of FPC antennas has been recently proposed [11]. An optimized double layer PRS FPC antenna has been presented which achieves a significant bandwidth enhancement compared to a single layer PRS FPC antenna. The antenna performance is related to the reflection characteristics of the PRS array using a simple ray optics model. According to this model, maximum directivity at boresight is obtained when constructive interference occurs i.e. when the resonance condition given in equation (1) is satisfied, where ϕ is the phase of the reflection coefficient of the PRS, h is the distance between the ground plane and the screen and λ_0 is the wavelength in free space.

$$\phi = \frac{4\pi h}{c} f - (2N-1)\pi, \qquad N = 0,1,2... \quad (1)$$

It can be seen from this equation that in order to obtain maximum directivity over a broad frequency range, a linearly increasing PRS reflection phase response with frequency is desired. This was first achieved in [11], using a double-layer array of square metallic patch arrays with dissimilar array element dimensions. Later, in [12] a double-layer square ring defected geometry was presented obtaining an increasing phase. More recently, a positive phase gradient was achieved employing dipoles printed on both sides of a dielectric

substrate [13]. In all the above cases the antenna radiation bandwidth has been enhanced, validating the conclusions of equation (1). Furthermore, in [14-16] directivity enhancement was achieved employing multiple EBG superstrates and an array of multiple sources instead of a single source.

In this paper, we present for the first time the design and implementation of a three-layer PRS for enhancement of the directivity – bandwidth (BW) product of FPC antennas and thereby generalize the concept of broadband FPC antennas with multiple PRS layers. In addition we present a simple equivalent circuit model for the design of the proposed multi-layer PRSs.

The proposed antenna configuration is shown in Fig. 1. A three-layer PRS is studied and optimized to produce a reflection phase increasing with frequency over a wide range by virtue of the resonances of the two cavities formed between the three PRSs. An equivalent circuit approach using AWR Microwave office™ is initially employed and periodic full wave simulations are subsequently carried out in CST Microwave Studio™ in order to optimize the design of the PRS. Based on the optimized PRS designs, finite size FPC antennas are produced. A prototype antenna has been fabricated and measured.

The paper is organized as follows. In Section II an equivalent circuit model and a short description for periodic analysis is presented. In section III a parametric study and optimization for the design of the three PRS layers is carried out.. In section IV simulation and measurement results of a finite size three-layer antenna are presented.

II. Unit Cell Topology and Equivalent Circuit Model

Multi-layer PRS arrays are studied in this section using an equivalent circuit approach which allows for a fast optimization of the design. Each layer consists of a metallic square patch PRS array printed on a 1.6mm thick dielectric substrate with permittivity ε_r=2.55.

In order to demonstrate the equivalent circuit approach and its accuracy in modelling the proposed multi-layer PRSs working examples of a single-layer, a two-layer and a three-layer PRS are employed. The three-layer design is based on the optimised design that is produced later on in section III. The unit cell dimensions, as shown in Fig. 1(a) and starting from the layer closer to the ground plane, are d_1=9.16mm, d_2=10mm and d_3=6mm. The periodicity for all three layers is P=11mm. Finally the cavity distances are h_1=9.5mm and h_2=10mm. The above dimensions have been chosen after investigations explained in Section III.

The unit cell of a periodic metallic patch array printed on a dielectric substrate can be modeled with the equivalent circuit shown in Fig. 2(a) [17, 18]. In order to model the metallic patches as equivalent electrical parameters, the electric and magnetic fields should be considered. Strong electric field is generated on the surface of the metallic patches due to electromagnetic excitation. The established electric field between two adjacent elements causes a capacitive behavior and is modeled with a shunt capacitor C_i. The inductor in series L_i represents the current flowing through the patches. The dielectric substrate can be modeled as a transmission line with the length of the line t_i being equal to the substrate's thickness and the characteristic impedance is calculated from $Z_i = Z_0 / \sqrt{\varepsilon_r}$, Z_0=377 Ω is the free space impedance and ε_r is the dielectric constant of the material. The two terminals represent the free space on both sides of the PRS and have characteristic impedance equal to Z_0.

An initial calculation of the electrical parameters C_i and L_i from the physical dimensions of the unit cell can be realized using equations (3) and (4) [19] where P is the periodicity, $s=P-d$ is the separation between two adjacent patches, d is the width of the patch and $\varepsilon_{eff}= \varepsilon_r$.

$$C = \varepsilon_0 \varepsilon_{eff} \frac{2P}{\pi} \ln\left(\frac{1}{\sin\left(\frac{\pi s}{P}\right)} \right) \quad (3)$$

$$L = \mu_0 \frac{P}{2\pi} \ln\left(\frac{1}{\sin\left(\frac{\pi d}{2P}\right)} \right) \quad (4)$$

For multiple layer structures, the equivalent circuit of each layer is cascaded, adding a transmission line to model the air cavity between the layers. The length of the line is equal to the cavity distance and the impedance is the one of the free space. In Fig. 2(b) the three-layer equivalent circuit is presented.

To validate the model the complex reflection coefficients have been obtained for single, double and three-layer PRS using both circuit analysis software (AWR Microwave Office) and full-wave simulations (CST Microwave Studio). In CST, periodic boundary conditions are applied to the unit cell of the structure, which assume an infinite extend of the surface, and reduce the calculations of the complete structure into a single unit cell. Simulations have been carried out for six different values of the physical dimension of the patch (d) for a single PRS. Different combinations were then investigated for double and three-layer PRSs. In Fig. 3 one case for a single, a double and a three-layer PRS is shown for brevity.

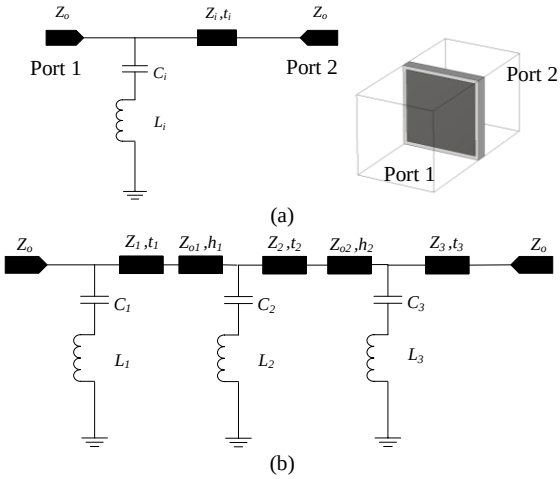

Fig. 2. Equivalent circuit for (a) single-layer PRS, (b) three-layer PRS.

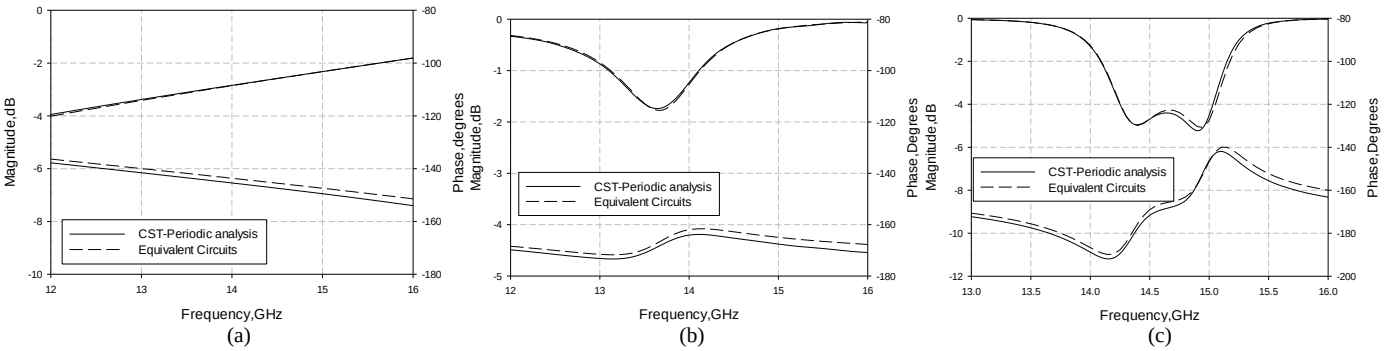

Fig. 3. Complex Reflection Coefficients for (a) single-layer PRS for d=6mm, (b) double-layer PRS for d_1=10mm, d_2=6mm and h_1=11mm, (b) three-layer PRS for the proposed design dimensions, obtained from the equivalent circuit model and periodic full-wave analysis.

TABLE I
PHYSICAL AND ELECTRICAL PARAMETERS FOR SINGLE-LAYER PRS

d (mm)	C (pF)	L (nH)
10	0.2101	0.088
9.16	0.1301	0.27
9	0.1251	0.263
8	0.0751	0.66
7	0.0481	1.14
6	0.0292	1.959

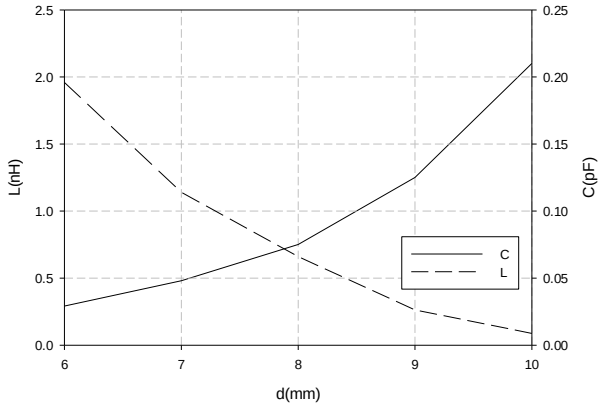

Fig. 4. Variation of equivalent capacitance and inductance with the physical dimension of the PRS.

Good agreement has been achieved after fine tuning of the values obtained from equations (3) and (4) of the electrical parameters (Fig. 3). The values used for C and L are presented in Table I. The good agreement can be attributed to the fact that the separation between the layers in the proposed design is in the order of half wavelength, hence the effects of the higher order evanescent Floquet harmonics are minimal.

In Fig. 4 the variation of the equivalent capacitance and inductance as the patch dimensions increase is depicted. It is evident that increasing the patch size, leads to increased capacitance and reduced inductance. This behavior can be justified taking into account that as the patch increases the separation between the adjacent elements decreases causing an increase of the electric coupling. On the other hand, decreasing the patch dimension, the induced currents become stronger leading to larger inductance values.

III. DESIGN OF THREE LAYER PRS

In this section a parametric study and optimization of a three layer PRS is carried out with the aim of achieving a reflection phase response increasing with frequency within the desired operating frequency of the FPC antenna.

As mentioned in the introduction a positive gradient in the phase of the reflection coefficient with frequency is required to achieve high gain for a broad frequency range. The values of the parameters for the desired behavior in the phase of the reflection coefficient i.e. approaching the optimum phase derived from equation (1) were found after a parametric optimization procedure. It should be noted that the ground plane is not included in the complex reflection coefficients calculations, so only two cavities are formed. Nevertheless, for the derivation of the optimum phase the distance h between the ground and the first layer is needed, and was selected to be h=10.7mm.

Two resonances are obtained from the three-layer PRS. At each resonant frequency the magnitude of the reflection coefficient has a minimum and the phase is increasing for a frequency range around the resonance. To achieve a broadband phase increase the two resonances have to be brought close together but not overlap.

In Fig. 5 and Fig. 6 the complex reflection coefficients are presented for three different values of each of the structure's parameters and the optimum phase is also included. The optimized case for the selected values is shown as a reference in all the graphs (solid line). In the optimized case, two minimums occur in the reflection magnitude at 14.4GHz and 14.9GHz. An increase in the positive gradient range of the phase is obtained, extending between 14.1GHz to 15.1GHz. This is a significant improvement over the optimized two-layer PRS case (see Fig. 3b). The positive gradient phase response leads to high antenna directivity in this frequency range according to the ray analysis, if the proposed PRSs are employed in the design of an FPC antenna. It is expected that at the frequencies where the optimized phase value is equal to that of the optimum phase, maximum directivity will be achieved since the cavity resonance condition, (1), is satisfied.

In Fig. 5(a, b) the effect of the two cavity heights is shown. It can be observed that the first cavity has a stronger effect than the second. Varying h_1 by half millimeter below and

above the selected value (h_1 =9.5mm) only one resonance occurs with a significant shift at higher or lower frequency respectively from the center frequency which is 14.6GHz. The same behavior is obtained with variation of h_2 but with a smaller frequency shift. In Fig. 6(a, b and c) the effect of the PRS size of each layer is studied. Variation in the size is much less significant than in the height of the cavities. As d_1 increases, although two resonances take place, the resonance at the lower frequency becomes dominant. For the selected value d_1=9.16mm, the two resonances have the same strength

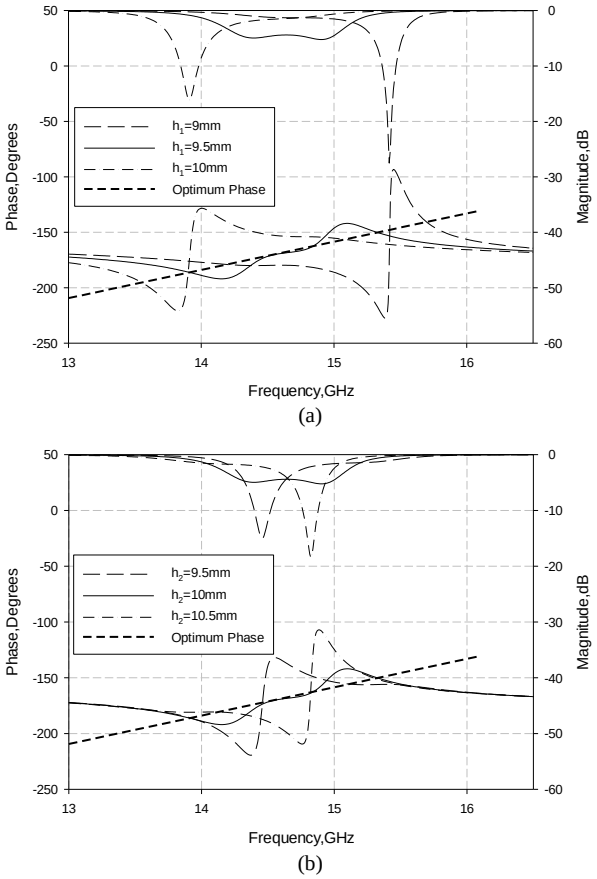

Fig. 5. Complex Reflection Coefficients of the three-layer PRS changing (a) the cavity distance h_1 (h_2=10mm, d_1=9.16mm, d_2=10mm, d_3=6mm), (b) the cavity distance h_2 (h_1=9.5mm, d_1=9.16mm, d_2=10mm, d_3=6mm).

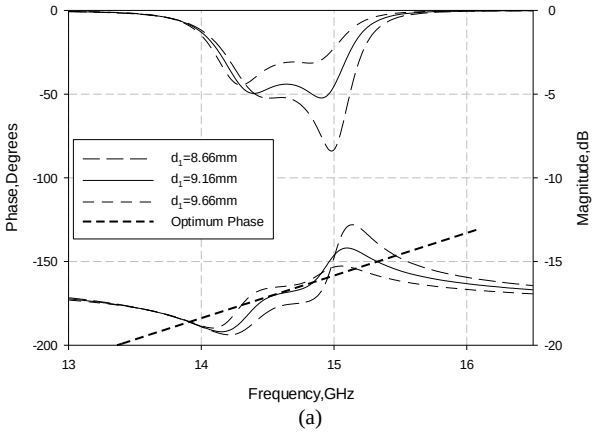

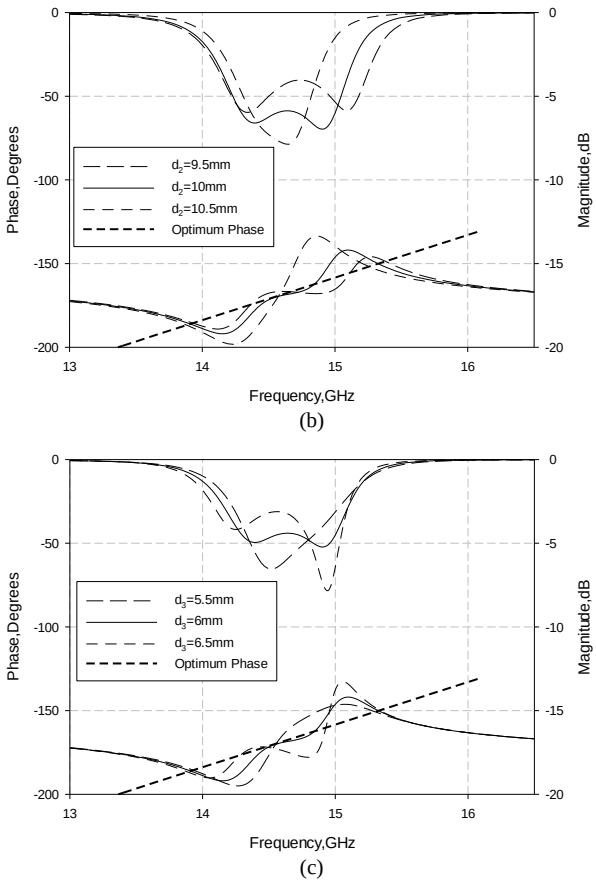

Fig. 6. Complex Reflection Coefficients of the three-layer PRS changing (a) the first layer patch dimensions d_1 (h_1=9.5mm, h_2=10mm, d_2=10mm, d_3=6mm), (b) the second layer patch dimensions d_2 (h_1=9.5mm, h_2=10mm, d_1=9.16mm, d_3=6mm) and (c) the third layer patch dimensions d_3 (h_1=9.5mm, h_2=10mm, d_1=9.16mm, d_2=10mm).

and the phase is closer to the optimum. For d_2, it is observed that for smaller values the two resonances move apart, while for larger values they overlap. Finally, when d_3 is increased the resonance at the higher frequency becomes stronger. For d_3=5.5mm the two resonances overlap again.

IV. Finite Size Antenna

In this section a realistic finite size antenna structure has been simulated based on the optimized designs obtained in the previous section. A comparison with an optimized two-layer antenna is presented in order to validate the improvement in the gain-bandwidth product by virtue of the proposed three-layer design. Measurements of a fabricated prototype of the proposed three-layer antenna are also presented.

The structure has been formed using the optimized three-layer PRS placed in front of a 1.6 mm thick metallic ground plane (Fig. 1(b)). A waveguide – fed slot inside the ground plane is used as a single feeder of the antenna. The dimensions of the slot are 10x2.5mm^2. The dimensions of the slot in the ground plane were selected such that a good matching in the frequency range of interest is achieved. The overall lateral dimensions of the antenna are 80x80mm^2, which corresponds to about 4λ at 14.5GHz. A total of 5x5 array elements are

printed on each dielectric layer. For this finite size structure, the distance *h* was changed to 11.3mm instead of 10.7mm which was used for an infinite size antenna. The rest of the parameters are h_1=9.5mm, h_2=10mm, d_1=9.16mm, d_2=10mm and d_3=6mm, as described in the previous section.

The antenna's simulated directivity is shown in Fig. 7 (solid line). A maximum directivity of around 21dBi is observed at 13.7GHz and it is kept over 18dBi for frequencies between 13.5GHz to 15.7GHz. The 3dB radiation bandwidth is calculated at approximately 15%. It is interesting to note that three peaks appear in the directivity of the antenna at three closely spaced frequencies corresponding to a third order cavity resonance response, which in turn is attributed to the three formed cavities. Moreover, these three peaks coincide with the frequencies where the resonant condition is satisfied, i.e. where the reflection phase of the PRSs crosses the optimum phase line (see Fig. 5). The directivity of an optimized two-layer antenna is also shown in Fig. 7. It has a directivity maximum of around 20dBi with a 3dB radiation bandwidth of 10.6%. Two peaks are observed in this case related to the resonances of the two cavities. It is evident that the three-layer antenna outperforms the two-layer one. In Table II a more detailed comparison between the two antennas is presented.

In Fig. 8, two other cases are compared with the optimized one, corresponding to different h_1=9mm and h_2=9.5mm. It can be observed that, after changing the first cavity distance, a deep drop occurs at 15.6GHz that deteriorates the antenna performance by significantly reducing the operating bandwidth. This behavior is justified from the corresponding reflection coefficient in Fig. 5(a). A similar effect is observed after reducing h_2 where the average directivity drops over the operating bandwidth compared with the optimized case, with a minimum of around 17dBi at 15GHz and the antenna bandwidth is thus significantly reduced. It should be noted that the radiation patterns in both of the above cases are also distorted at out-of-band frequencies (approximately over 15 GHz).

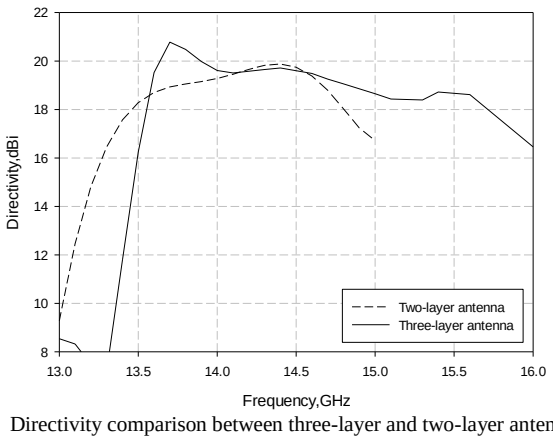

Fig. 7. Directivity comparison between three-layer and two-layer antenna.

TABLE II
COMPARISON BETWEEN DOUBLE LAYER AND THREE LAYER ANTENNA

Antenna Design	Maximum Directivity (dBi)	-3dB Radiation Bandwidth (%)	Directivity - Bandwidth Product
Double layer	19.88	10.6	1031
Three layer	20.8	15.1	1815

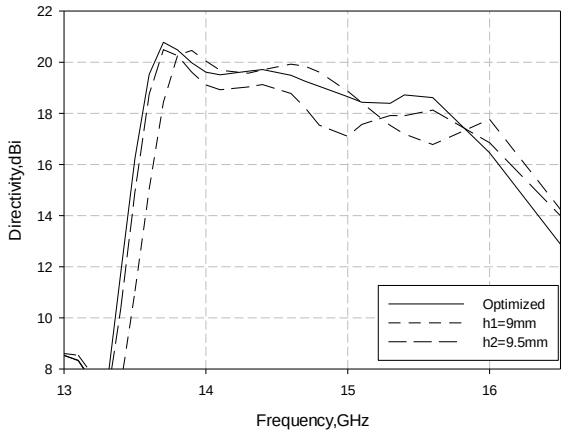

Fig. 8. Simulated directivity versus frequency for different cavity distances h_1 and h_2.

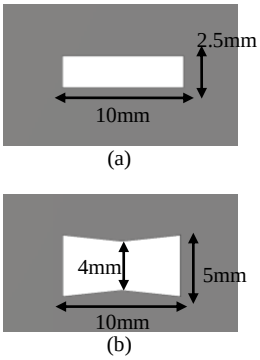

Fig. 9. Schematic diagram of the two slot designs: (a) Slot A and (b) Slot B.

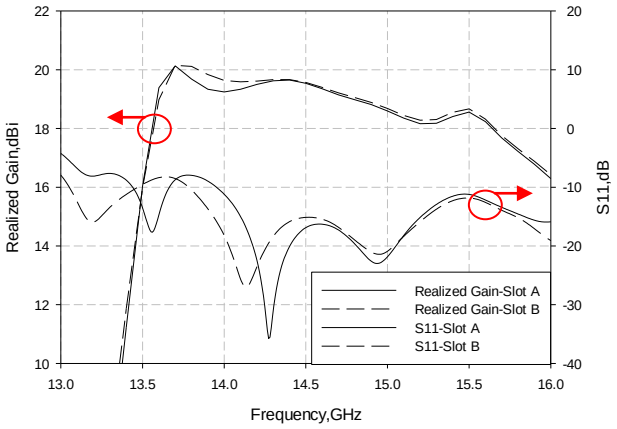

Fig. 10. Simulated S_{11} and gain for the two slot designs of Fig. 9.

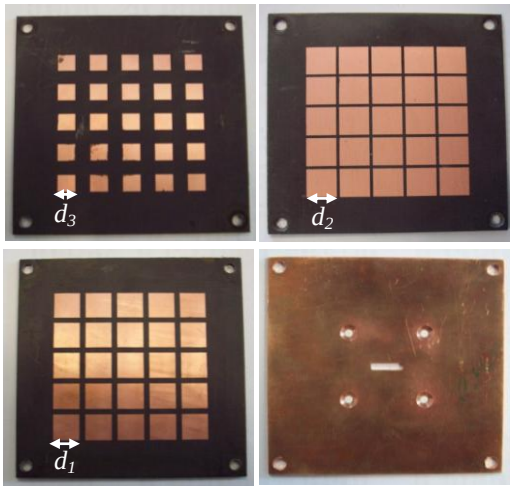

(a)

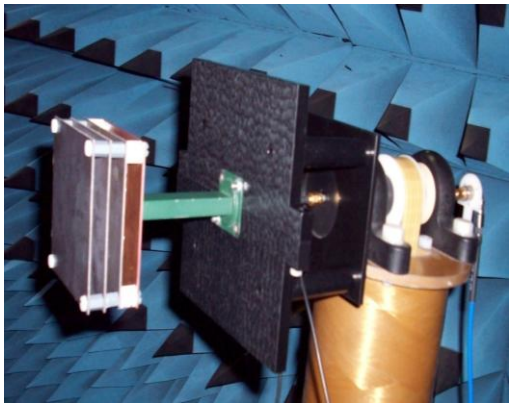

(b)

Fig. 11. Photograph of (a) three PRS layers and ground plane, (b) complete antenna.

Two shapes have been investigated for the feeding slot (Fig. 9), in order to achieve good matching, namely a simple rectangular slot with the dimensions mentioned in the beginning of this section (slot A) and a bow tie one (slot B). The simulated S11 and gain for both cases are shown in Fig. 10. It can be observed that slot B gives a slightly improved S11 and gain respectively. The antenna exhibits broadband performance with a maximum gain of 20dBi and bandwidth of 15%. There is a slight deterioration of the S11 assuming a maximum value of -8.5dB at approximately 13.7GHz. However this only reduces the gain at that frequency by less than 1dB (compared to the directivity).

Because of fabrication limitations, slot A has been selected for the final prototype. A prototype of the proposed antenna has been fabricated and measured in a full anechoic chamber (Fig. 11). Plastic screws and spacers were used for the mounting of the antenna. Due to fabrication inaccuracies the dimensions of the slot in the ground plane were 10.7x2.5mm^2 (instead of 10x2.5mm^2). The simulated and measured return loss of the antenna with the new slot dimensions is presented in Fig. 12. A minimum occurs at 13.95GHz, with satisfactory matching within the 3dB radiation bandwidth. At the edges of the band the measured matching deteriorates slightly due to

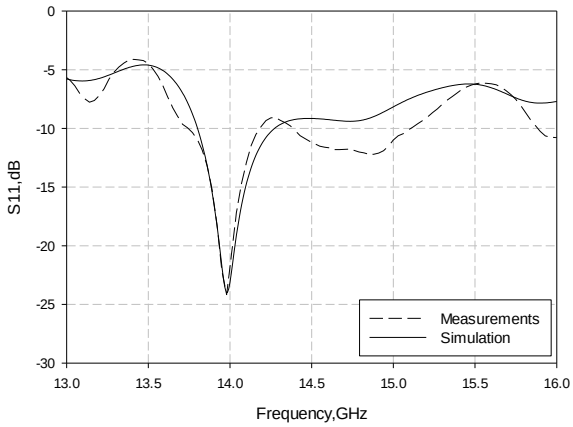

Fig. 12. Simulated and measured return loss for slot dimensions 10.7x2.5mm^2.

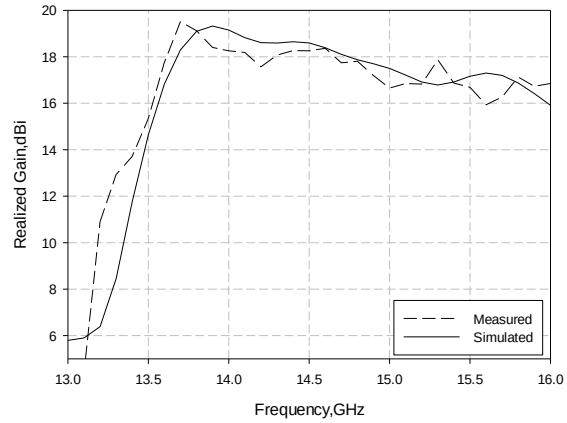

Fig. 13. Simulated and measured realized gain for the final antenna.

the narrowband operation of the feeding slot. Fig. 13 shows the simulated and measured gain versus frequency. A good agreement is obtained with a maximum measured value of 19.5dBi at 13.7GHz. The small discrepancy between simulation and measurement is attributed to fabrication tolerances. Moreover the well known gain transfer method was employed in order to measure the prototype antenna's gain which implies a ±0.5dB error introduced by the gain of the reference broadband horn antenna used. The gain values are approximately 1dB lower than the directivity values due to the imperfect matching and material losses.

The H- and E-plane patterns where measured in five different frequencies within the operating band. Simulated and measured results are presented in Fig. 14. In all frequencies the sidelobe level is below -10dB. There are some discrepancies between simulation and measurement especially at around 60^o. It was found that these are caused by the large plastic supporting base of the waveguide that can be seen in the photo of Fig. 11. The results presented here were obtained after a thin layer of absorbers were placed around the supporter behind the antenna which improved the sidelobe level at these angles by at least 3dBs compared to the patterns obtained without absorbers.

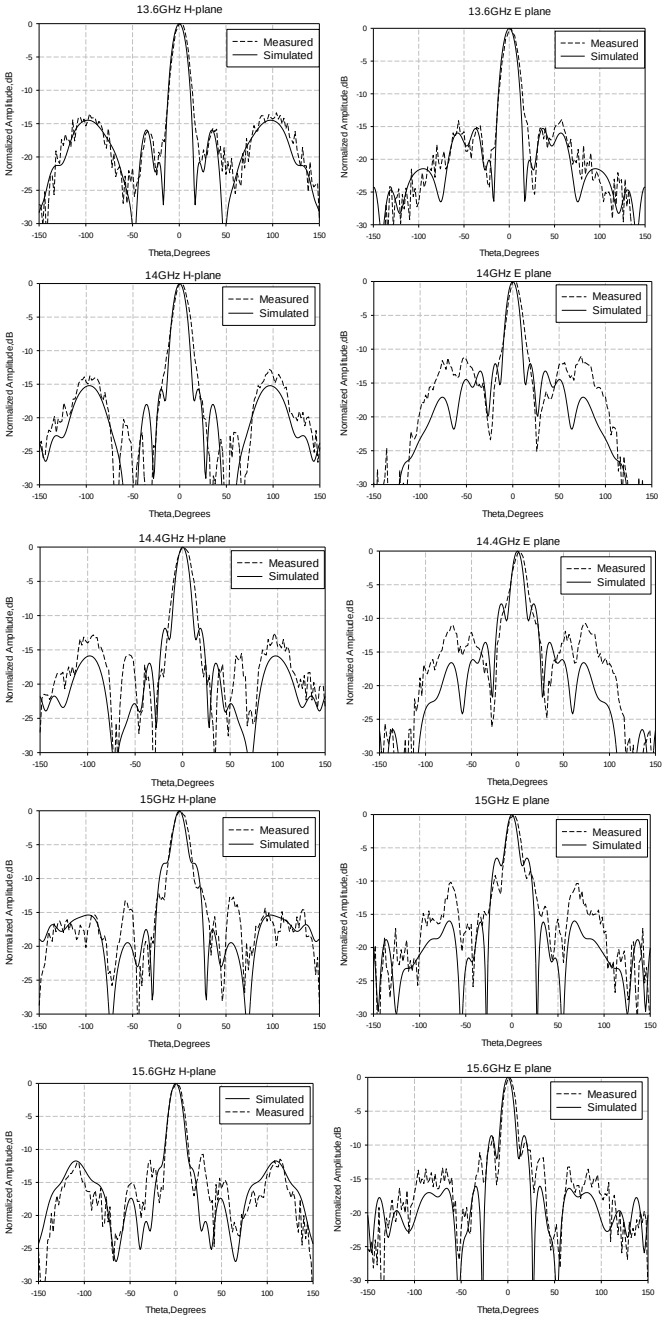

(a) (b)

Fig. 14. Simulated and measured patterns for the (a) H-plane and (b) E-plane in five frequencies over the operational bandwidth of the antenna.

V. CONCLUSION

Three-layer PRSs with reflection phase increasing with frequency over a wide range have been designed and presented. An equivalent circuit model was employed successfully for the PRS design. A high gain broadband Fabry-Perot type antenna was proposed, based on the optimized PRSs. The three layers of PRSs were printed on thin dielectric substrates of the same thickness and placed in front of a ground plane, forming three open cavities. An antenna of around 20 dBi gain at a central operating frequency of 14.5 GHz has been design with a 3dB bandwidth of about 15%, outperforming earlier antenna designs based on two–layer PRS. Measured results of a fabricated prototype have been presented and are in good agreement with simulation predictions.

REFERENCES

[1] G.V. Trentini, "Partially reflecting sheet array", *IRE Trans. Antennas Propag.*, vol. AP-4, pp. 666-671, 1956.

[2] A. P. Feresidis, and J. C. Vardaxoglou, "High-gain planar antenna using optimized partially reflective surfaces," *IEE Proc. Microw. Antennas Propag.*, vol. 148, no. 6, Feb. 2001.

[3] J. R. James, and P. S. Hall, *Handbook of microstrip antennas*, Peter Peregrinus Ltd., 1989.

[4] Y. J. Lee, J. Yeo, R. Mittra, and W. S. Park, "Design of a high-directivity electromagnetic bandgap (EBG) resonator antenna using a frequency selective surface (FSS) superstrate," *Microwave and Optical Technology Letters*, vol. 43, no. 6, pp. 462-467, Dec. 2004.

[5] T. Zhao, D. R. Jackson, J. T. Williams, Hung-Yu D. Yang, and A. A. Oliner, "2-D Periodic Leaky-Wave Antennas-Part I: Metal Patch Design", *IEEE Trans. Antennas and Propag.*, vol. 53, no. 11, pp.3505-3514, Nov. 2005.

[6] T. Zhao, D. R. Jackson, J. T. Williams, Hung-Yu D. Yang, and A. A. Oliner, "2-D Periodic Leaky-Wave Antennas-Part II: Slot Design", *IEEE Trans. Antennas and Propag.*, vol. 53, no. 11, pp. 3515-3524, Nov. 2005.

[7] A. Oliner. "Leaky-wave antennas," in Antenna Engineering Handbook, Third Edition, edited by *R. C. Johnson, McGraw Hill*, 1993.

[8] A. P. Feresidis, G. Goussetis, S. Wang, and J. C. Vardaxoglou, "Artificial Magnetic Conductor Surfaces and Their Application to Low-Profile High- Gain Planar Antennas," *IEEE Trans. Antennas Propag.*, vol. 53, no. 1, pp. 209-215, Jan. 2005.

[9] S. Wang, A.P. Feresidis, G. Goussetis, J.C. Vardaxoglou, "High-Gain Subwavelength Resonant Cavity Antennas Based on Metamaterial Ground Planes," *IEE Proc. Antennas and Propagation*, Vol. 153, no. 1, pp.1-6, February 2006.

[10] J. R. Kelly, T. Kokkinos, and A. P. Feresidis, "Analysis and Design of Sub-wavelength Resonant Cavity Type 2-D Leaky-Wave Antennas," *IEEE Trans. Antennas and Propagation*, vol. 56, no. 9, pp. 2817-2825, Sept. 2008.

[11] A. P. Feresidis, J. C. Vardaxoglou, "A broadband high-gain resonant cavity antenna with single feed", *Proc. EuCAP* 2006, Nice, France, 2006.

[12] L. Moustafa and B. Jecko, "EBG structure with wide defect band for broadband cavity antenna applications," *IEEE Antenna Wireless Propagat. Lett.*, vol.7, pp.693-696, Nov.2008.

[13] Ge Yuehe, K.P. Esselle, and T.S. Bird, "The Use of Simple Thin Partially Reflective Surfaces With Positive Reflection Phase Gradients to Design Wideband, Low-Profile EBG Resonator Antennas ", *IEEE Trans. Antennas Propag.*, vol. 60, no. 2, pp. 743-750, Feb. 2012.

[14] Y.J. Lee, J. Yeo, R. Mittra, and W. S. Park, "Application of electromagnetic bandgap (EBG) superstrates with controllable defects for a class of patch antennas as spatial angular filters," IEEE Trans. Antennas Propagat., vol. 53, no. 1, pp. 224-235, Jan. 2005.

[15] R. Gardelli, M. Albani, F. Capolino, "Array thinning by using antennas in a Fabry-Perot cavity for gain enhancement," Antennas and Propagation, IEEE Transactions on , vol.54, no.7, pp.1979-1990, July 2006.

[16] A.R.Weily, K.P. Esselle, T.S. Bird and B.C. Sanders, "Dual resonator 1-D EBG antenna with slot array feed for improved radiation bandwidth," IET Microwaves, Antennas Propagat., vol. 1, no. 1, pp. 198-203, February 2007.

[17] B. A. Munk, Frequency Selective Surfaces: Theory and Design. New York: Wiley-Interscience, 2000.

[18] B. A. Munk, Finite Antenna Arrays and FSS. New York: Wiley-Interscience, 2003.

[19] N. Marcuvitz, *Waveguide Handbook.* Lexington, MA: Boston Technical, 1964, pp.218-285.

Konstantinos Konstantinidis was born in Thessaloniki, Greece in 1985. He received the B.Sc. in physics and the M.Sc. degree in electronics physics (Radioelectrology - Telecommunications Division) from the Aristotle University of Thessaloniki (AUTh) in 2007 and 2009 respectively.

Since 2011, after his military service, he has been working toward the Ph.D. degree in the School of Electronics, Electrical and Computer Engineering, University of Birmingham, Edgbaston, Birmingham, U.K. His research interests mainly focus on high-gain planar metamaterial-based antennas.

Alexandros P. Feresidis (S'98-M'01-SM'08) was born in Thessaloniki, Greece, in 1975. He received the Physics degree from Aristotle University of Thessaloniki, Greece, in 1997, and the MSc(Eng) in Radio Communications and High Frequency Engineering from the University of Leeds, UK, in 1998. In 2002, he obtained the Ph.D. in Electronic and Electrical Engineering from Loughborough University, UK.

During the first half of 2002, he was a research associate and in the same year he was appointed Lecturer in Wireless Communications in the Department of Electronic and Electrical Engineering, Loughborough University, UK, where, in 2006, he was promoted to Senior Lecturer. In December 2011 he joined the School of Electronic, Electrical and Computer Engineering, University of Birmingham, UK. He has published more than 100 papers in peer reviewed international journals and conference proceedings and has co-authored three book chapters. His research interests include analysis and design of artificial periodic metamaterials, electromagnetic band gap (EBG) structures and frequency selective surfaces (FSS), leaky-wave antennas, small/compact antennas, numerical techniques for electromagnetic, passive microwave/mm-wave circuits and bioelectromagnetics.

Dr Feresidis holds a Senior Research Fellowship from the U.K. Royal Academy of Engineering and The Leverhulme Trust (2013-2014).

Peter S. Hall (M'88–SM'93–F'01) is Professor of Communications Engineering, leader of the Antennas and Applied Electromagnetics Laboratory, and Head of the Devices and Systems Research Centre in the Department of Electronic, Electrical and Computer Engineering at The University of Birmingham. After graduating with a PhD in antenna measurements from Sheffield University, he spent 3 years with Marconi Space and Defence Systems, Stanmore working largely on a European Communications satellite project. He then joined The Royal Military College of Science as a Senior Research Scientist, progressing to Reader in Electromagnetics. He joined The University of Birmingham in 1994. He has researched extensively in the areas of antennas, propagation and antenna measurements. He has published 5 books, over 350 learned papers and taken various patents. These publications have earned many awards, including the 1990 IEE Rayleigh Book Award for the Handbook of Microstrip Antennas.

Professor Hall is a Fellow of the IEE and the IEEE and a past IEEE Distinguished Lecturer. He is a past Chairman of the IEE Antennas and Propagation Professional Group and past coordinator for Premium Awards for IEE Proceedings on Microwave, Antennas and Propagation. He is a member of the IEEE AP-S Fellow Evaluation Committee. He chaired the 1997 IEE ICAP conference, was vice chair of EuCAP 2008 and has been associated with the organization of many other international conferences. He was Honorary Editor of IEE Proceedings Part H from 1991 to 1995 and currently on the editorial board of Microwave and Optical Technology Letters. He is a past member of the Executive Board of the EC Antenna Network of Excellence.